CCS Chemistry

RESEARCH ARTICLE

Received: May 15, 2026 | Accepted: July 21, 2026 | Published: Sept. 16, 2026

Formal Aldehyde Insertion into C–S Bonds of Sulfones Enables Modular Synthesis of Tetrasubstituted *gem*-Bis(trifluoromethyl) Alkenes

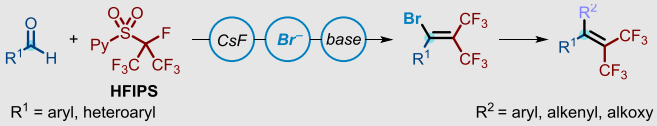
Feng Zhao[1,2], Kaidi Zhu[2], Yunlong Zhao[2], Lin Xiao[2], Fu Chen[2], Yu He[2], Xiu Wang[2], Mingyou Hu[2], Chuanfa Ni[2]* & Jinbo Hu[1,2]*

[1]*College of Chemistry, Central China Normal University, Wuhan City, Hubei 430079,* [2]*State Key Laboratory of Fluorine and Nitrogen Chemistry and Advanced Materials, Shanghai Institute of Organic Chemistry, University of Chinese Academy of Sciences, Chinese Academy of Sciences, Shanghai City, Shanghai 200032*

**Corresponding author: jinbohu@sioc.ac.cn; nichuanfa@sioc.ac.cn*

Cite this: *CCS Chem*. **2026**, Just Published. DOI: 10.31635/ccschem.026.202608038

Nucleophile-triggered activation of fluoroalkyl sulfones offers a potential entry to fluorinated building blocks, yet formal carbonyl insertion into C–S bonds of sulfones remains largely unexplored due to stringent structural and electronic constraints. Herein, we report that heptafluoroisopropyl 2-pyridyl sulfone (HFIPS) uniquely enables efficient formal insertion of aldehyde into C–S bonds of sulfones under mild fluoride catalysis. Mechanistic investigations, supported by stoichiometric experiments and density functional theory analysis, identify the nucleophilic addition to aldehyde as the rate-determining step and establish HFIPS as the predominant sulfonylating species under turnover conditions. The resulting sulfonate intermediates are converted through a mechanistically indispensable bromination-elimination sequence, providing streamlined access to tetrasubstituted bromo-*gem*-bis(trifluoromethyl) alkenes. The bromo substituent serves as a versatile handle for modular downstream functionalization. Structural and photophysical studies reveal that geminal CF_3 groups impose steric restriction and suppress intramolecular rotation, thus enhancing the aggregation-induced emission behavior in tetraphenylethene-derived systems. This unified platform integrates formal C–S insertion chemistry with fluorinated alkene synthesis and functional materials design.



Keywords: **aldehyde, sulfone, tetrasubstituted alkene, *gem*-bis(trifluoromethyl), olefination**

Introduction

Alkenes are ubiquitous structural motifs in natural products, pharmaceuticals, and functional materials, where their geometry and substitution patterns often exert a profound influence on molecular properties and performance.[1,2] Consequently, the development of versatile carbonyl olefination strategies has remained a central pursuit in synthetic chemistry, enabling precise control over substitution patterns and providing efficient access to structurally diverse alkenes.[3–5] Among established approaches, the Julia–Kocienski olefination has emerged as a robust approach for the synthesis of tetrasubstituted alkenes from ketones, benefiting from high efficiency and

Citation: *CCS Chem*. **2026**, Just Published. DOI: 10.31635/ccschem.026.202608038
Link to VoR: https://doi.org/10.31635/ccschem.026.202608038

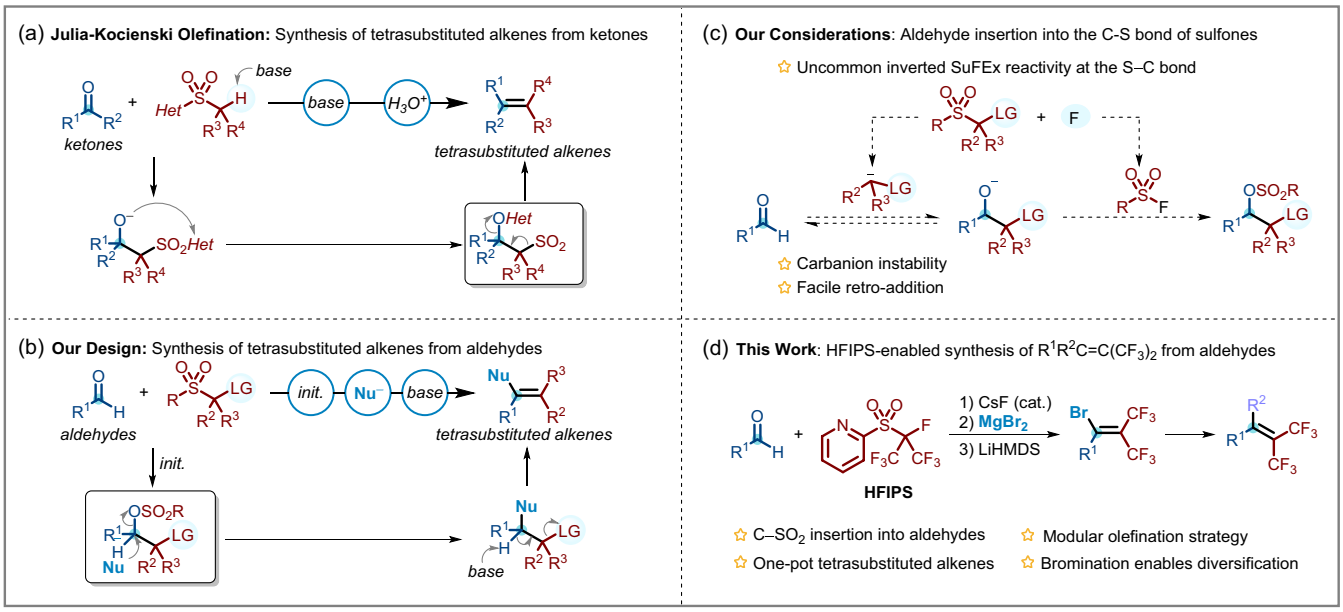


Figure 1 | *Background and reaction design. Het = heteroaryl. (a) Julia–Kocienski olefination: synthesis of tetrasubstituted alkenes from ketones; (b) our design: synthesis of tetrasubstituted alkenes from aldehydes; (c) our considerations: aldehyde insertion into the C–S bond of sulfones; and (d) this work: HFIPS-enabled synthesis of* $R^1R^2C = C(CF_3)_2$ *from aldehydes.*

broad substrate scope[6–8] (Figure 1a). In contrast, aldehydes afford, at most, trisubstituted alkenes[9] to support recent advances in the Julia–Kocienski olefination for the synthesis of trisubstituted alkenes, because the corresponding heteroaryloxy-substituted sulfinate intermediates readily undergo desulfination–elimination under standard conditions rather than proceeding through a substitution pathway.[10–12] As a result, access to tetrasubstituted alkenes from aldehydes remains limited in current carbonyl olefination methodologies.

To address this limitation, we envisioned a complementary strategy based on the formal incorporation of aldehydes into the C–S bond of a suitably designed (hetero) aryl sulfone (Figure 1b). By introducing an appropriate leaving group on the alkyl fragment to modulate sulfone reactivity,[13–18] the resulting sulfonate intermediate could serve as a platform for subsequent conversion into tetrasubstituted alkenes. Conceptually, this approach enables modular assembly of aldehyde, sulfone, and nucleophile components. Mechanistically, fluoride activation of a (hetero)aryl sulfone generates a reactive carbanion species that can be captured by aldehydes, ultimately affording a sulfonate intermediate through sulfonyl transfer (Figure 1c).[19–22] Subsequent functionalization of this intermediate would provide access to structurally diverse tetrasubstituted alkene.

Several challenges must be overcome to realize this strategy. First, heterolytic C–S bond cleavage via fluoride attack at sulfur—formally the reverse of a SuFEx process[23]—is uncommon in conventional sulfones and observed mainly in highly activated or strained systems.[24–29] Second, the resulting trisubstituted carbanion intermediate may undergo rapid α-elimination,[30–33] limiting productive aldehyde capture. Third, the steric and electronic demands associated with this intermediate may impede aldehyde addition and promote retro-addition pathway,[7,34–36] thereby suppressing sulfonate formation.

To overcome these challenges, we designed a previously unreported heptafluoroisopropyl 2-pyridyl sulfone (HFIPS) reagent. The strongly electron-withdrawing heptafluoroisopropyl group finely tunes the electronic properties of the sulfone to enable the C–S addition to aldehydes, while the 2-pyridylsulfonate fragment serves as an effective leaving group for downstream transformations.[37] We anticipated that this reagent design would provide access to synthetically useful sulfonate intermediates that could be converted into tetrasubstituted alkenes under mild conditions.

Herein, we report a HFIPS-enabled aldehyde olefination strategy that furnishes tetrasubstituted bromo-*gem*-bis(trifluoromethyl) alkenes from readily available aldehydes and sulfone reagents (Figure 1d). The resulting bromo substituent serves as a versatile synthetic handle for cross-coupling and nucleophilic substitution, providing access to unsymmetrical and functionalized tetrasubstituted *gem*-bis(trifluoromethyl) alkenes, including derivatives exhibiting enhanced aggregation-induced emission (AIE) properties. The *gem*-bis(trifluoromethyl) alkene moiety has also been associated with distinctive

Citation: *CCS Chem.* **2026**, Just Published. DOI: 10.31635/ccschem.026.202608038
Link to VoR: https://doi.org/10.31635/ccschem.026.202608038

biological properties, including reported contraceptive activity in warm-blooded animals.[38] This modular platform enables efficient aldehyde olefination to access tetrasubstituted alkenes under mild, transition-metal-free conditions with broad functional-group tolerance.

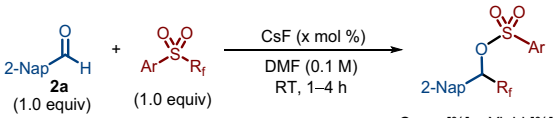
Experimental Methods

General procedures for one-pot olefination of aldehydes to access bromo-*gem*-bis(trifluoromethyl) alkenes 5

A sealed tube was charged with HFIPS **1** (0.50 mmol) and aldehyde **2** (0.50 mmol) under N_2 atmosphere. CsF (0.10 mmol, 15.2 mg) and CH_3CN (5.0 mL) were added in a nitrogen-filled glovebox. The mixture was stirred at room temperature for 4 h. $MgBr_2$•Et_2O (1.00 mmol) was added under N_2 atmosphere. The mixture was stirred at 80 °C for 12 h. When the reaction was completed, the mixture was filtered, then the filtrate was concentrated in vacuo. Et_2O (10.0 mL), HMPA (1.0 mL), and a solution of LiHMDS (0.60 mmol) in Et_2O (3.0 mL) were added via a gastight syringe under a nitrogen atmosphere. The mixture was stirred at 0 °C for 30 min. The reaction was monitored by ^{19}F NMR spectroscopy or TLC. When the reaction was completed, the mixture was quenched with H_2O (20 mL) and extracted with Et_2O (20 mL × 3). The organic phase was dried over anhydrous Na_2SO_4, and the solvent was concentrated in vacuo. The crude product was purified by silica gel column chromatography using petroleum ether/ethyl acetate as the eluent. More experimental details and characterization are available in the (Supporting Information Figures S5, S14–S55, and Table S4).

General procedures for the Suzuki–Miyaura cross-coupling of bromo-*gem*-bis(trifluoromethyl) alkenes 5 to access 8

A sealed tube was charged with bromo-*gem*-bis(trifluoromethyl) alkenes **5f** (0.10 mmol, 46.3 mg) and aryl or alkenyl boric acid **10** (0.15 mmol) under N_2 atmosphere. $Pd_2(dba)_3$ (0.0025 mmol, 2.3 mg), TDMPP (0.01 mmol, 4.4 mg), and K_3PO_4 (0.30 mmol, 63.7 mg) were added in a nitrogen-filled glovebox. $PhCH_3$ (1.0 mL) and H_2O (0.25 mL) were added via a gastight syringe under a nitrogen atmosphere. The mixture was stirred at 110 °C for 12 h. When the reaction was completed, the mixture was quenched with H_2O (5 mL) and extracted with Et_2O (5 mL × 3). The organic phase was dried over anhydrous Na_2SO_4, and the solvent was concentrated in vacuo. The crude product was purified by silica gel column chromatography using petroleum ether/ethyl acetate as the eluent. More experimental details and characterization are available in the (Supporting Information Schemes S2–S3, and Figures S56–S70).



	x	Conv. [%]	Yield [%]
Ar = Ph or Py, R_f = CF_3 or C_2F_5	100	0	0
Ar = Ph, R_f = $C(CF_3)_3$	100	>99	0
Ar = Ph, R_f = $CF(CF_3)_2$	100	>99	83
Ar = Py, R_f = $CF(CF_3)_2$ (**1**)	20	>99	>99

Scheme 1 | *Reactivity evaluation of representative fluoroalkyl sulfones. Conversions and yields were determined by ^{19}F NMR analysis. Nap = naphthyl; Py = 2-pyridyl; Ar = aryl; Ph = phenyl; DMF =* N,N*-dimethylformamide; RT = room temperature*

General procedures for the nucleophilic substitution of bromo-*gem*-bis(trifluoromethyl) alkenes 5 to access 9

A sealed tube was charged with bromo-*gem*-bis(trifluoromethyl) alkenes **5f** (0.10 mmol, 46.3 mg) under N_2 atmosphere. Sodium salt **11** (0.10 mmol) and THF (2.0 mL) were added in a nitrogen-filled glovebox. The mixture was stirred at room temperature for 10 h. When the reaction was completed, the mixture was quenched with H_2O (5 mL) and extracted with Et_2O (5 mL × 3). The organic phase was dried over anhydrous Na_2SO_4, and the solvent was concentrated in vacuo. The crude product was purified by silica gel column chromatography using petroleum ether/ethyl acetate as the eluent. More experimental details and characterization are available in the (Supporting Information Figures S71–S74).

Results and Discussion

Enabling formal insertion of aldehydes into the C–S bonds of sulfones

We began by evaluating formal insertion of aldehyde into the C–S bond of representative fluoroalkyl sulfones as the pivotal step toward tetrasubstituted olefins (Scheme 1). Despite literature precedent for nucleophilic activation of fluoroalkyl sulfones,[13,17] trifluoromethyl- and pentafluoroethyl-substituted aryl and heteroaryl sulfones proved entirely unreactive under fluoride activation. No sulfonate formation was detected, even in the presence of strong alkoxide bases.[39,40] Likewise, perfluoro-*tert*-butyl sulfones, although susceptible to fluoride-induced C–S cleavage,[24,25] failed to engage in formal insertion of aldehyde. These findings highlight the stringent steric and electronic requirements for formal C–S insertion and underscore the intrinsic difficulty of this transformation in conventional sulfone systems.

In sharp contrast, heptafluoroisopropyl 2-pyridyl sulfone (HFIPS, **1**) displayed distinctive and robust reactivity.

Citation: *CCS Chem.* **2026**, Just Published. DOI: 10.31635/ccschem.026.202608038
Link to VoR: https://doi.org/10.31635/ccschem.026.202608038

Under catalytic CsF (20 mol %) in anhydrous *N*,*N*-dimethylformamide (DMF) at room temperature, reaction with 2-naphthaldehyde (**2a**) furnished sulfonate ester in quantitative yield (^{19}F NMR) (for details, see the Supporting Information Table S1). Phenyl-based analogs delivered significantly lower yields (83%), even under stoichiometric fluoride activation, underscoring the crucial role of the 2-pyridyl sulfone framework in enabling efficient formal insertion of aldehyde.

A broad range of aromatic and heteroaromatic aldehydes underwent smooth addition to afford sulfonates **3a–3n** in good to excellent yields (Scheme 2a) (for details, see Supporting Information Scheme S1 and Table S2). Functional groups including 2-pyrimidinyl (**3g**), morpholino (**3h**), bromo (**3k**, **3l**), iodo (**3j**), *tert*-butylthio (**3m**), and trifluoromethyl (**3f**) substituents were well tolerated. The structure of **3f** was unambiguously confirmed by single-crystal X-ray diffraction analysis (for details, see Supporting Information Figure S6 and Table S5),[41] revealing a pronounced intramolecular π–π stacking interaction between the pyridyl and aryl fragments. Treatment of 4,4′-biphenyldicarboxaldehyde with 2.0 equiv of HFIPS resulted in double addition at both carbonyl groups, furnishing **3i** in excellent yield. Aliphatic aldehydes were also competent substrates, affording the corresponding sulfonates in moderate yields, as exemplified by **3o** (60%). These results establish HFIPS as uniquely competent for fluoride-triggered formal insertion of aldehyde into C–S bonds.

Mechanistic elucidation of the fluoride-initiated pathway

To elucidate the origin of the unique reactivity of HFIPS toward aldehydes, combined experimental and computational studies were conducted (Figure 2). Treatment of HFIPS with CsF in the absence of aldehyde led to complete conversion into $PySO_2F$ (Figure 2a, Eq. 1, Supporting Information Figure S1), confirming efficient fluoride-induced C–SO_2 bond activation. Because both HFIPS and $PySO_2F$ coexist under catalytic CsF conditions, their relative reactivity toward the alkoxide intermediate was directly compared to identify the operative sulfonylating species. Notably, potassium *tert*-butoxide also initiated the reaction (Figure 2a, Eq. 2, Supporting Information Figure S2), albeit slightly less effectively than CsF, indicating that HFIPS itself can directly engage in the alcoholate sulfonylation step. Given the convenient preparation of potassium alkoxides, stoichiometric experiments employing a potassium ion as the counterion were performed to clarify the dominant sulfonylation pathway under catalytic conditions (Figure 2a, Eqs. 3 and 4, Supporting Information Figure S3 and S4). These studies revealed that HFIPS furnished the sulfonate ester in significantly higher yield than $PySO_2F$, demonstrating that HFIPS preferentially undergoes direct sulfonylation of the alkoxide under fluoride activation.

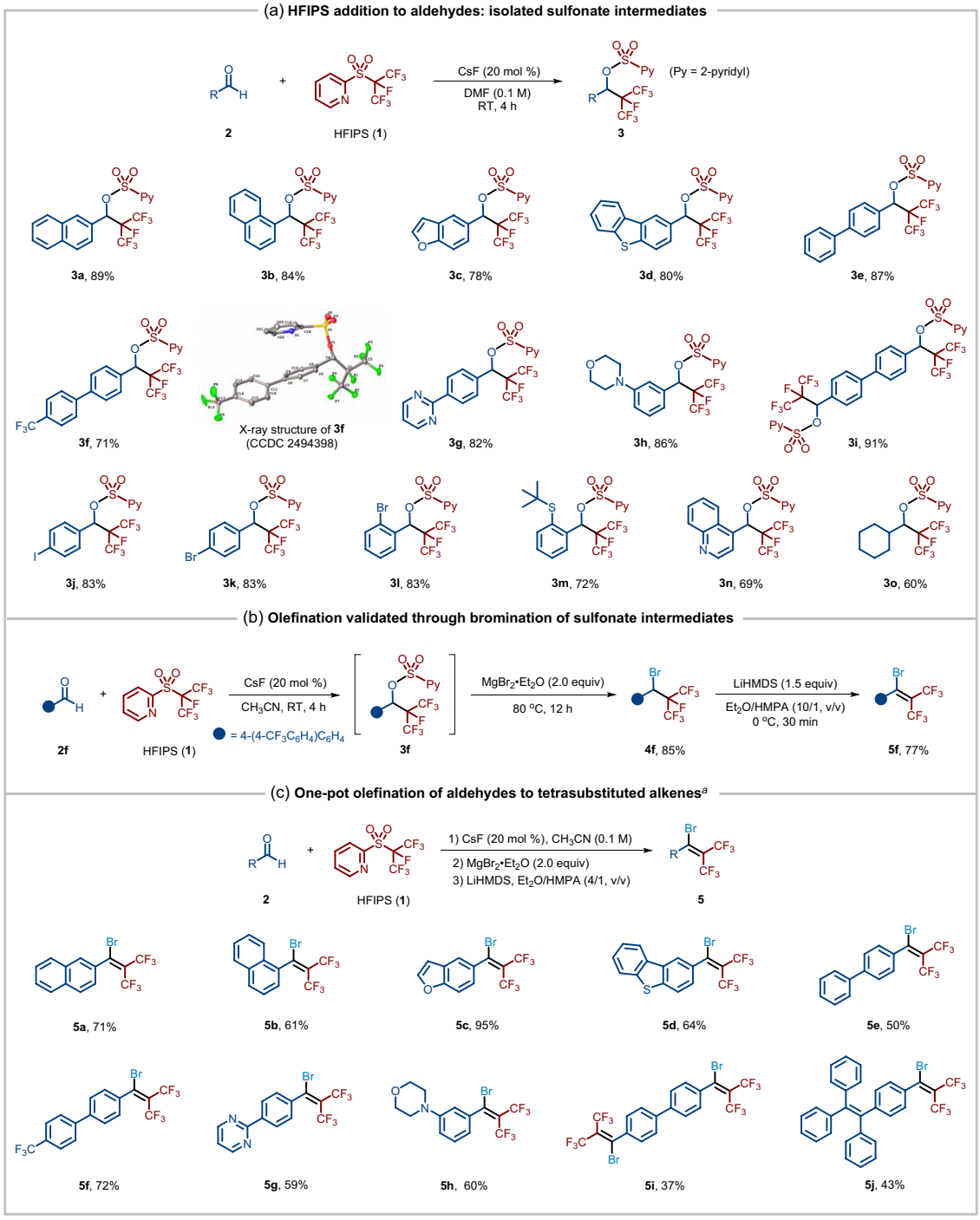
Based on these observations, two fluoride-initiated pathways can be envisioned (Figure 2b). Fluoride attack on HFIPS generates a hypervalent sulfur species, releasing $CF(CF_3)_2^-$ (**I**) and $PySO_2F$ (**6**). Nucleophilic addition of **I** to the aldehyde affords alkoxide intermediate **Int1**, which subsequently undergoes sulfonylation either with $PySO_2F$ to form sulfonate ester **3**, or directly with HFIPS, regenerating **I** in the process.

Density functional theory (DFT)-computed reaction profiles for the reaction of aldehyde **2b** with **I** (Figure 2c, Supporting Information Schemes S4–S8) identify nucleophilic addition as the rate-determining step [$\Delta G^{\ddagger}$(**TS1**) = +10.6 kcal · mol^{-1}; **int1** at +7.5 kcal · mol^{-1}]. In contrast, subsequent sulfonate formation proceeds through low-energy transition states with either HFIPS or $PySO_2F$ [$\Delta G^{\ddagger}$(**TS2-RF**) = +5.0 kcal · mol^{-1}; $\Delta G^{\ddagger}$(**TS3-F**) = +4.3 kcal · mol^{-1}], ultimately delivering the thermodynamically stable sulfonate **3** and regenerating **I** (–9.0 kcal · mol^{-1}). Although computation suggests a slightly lower barrier for sulfonylation via $PySO_2F$, experimental studies establish HFIPS as the predominant sulfonylating species. Overall, the reaction coordinate analysis demonstrates that the transformation is kinetically governed by the initial aldehyde addition, whereas sulfonate formation is fast and largely irreversible under the reaction conditions.

Overcoming steric constraints: olefination via bromination-elimination strategy

With sulfonate intermediates in hand, we sought to access tetrasubstituted alkenes via base-induced elimination. Direct elimination[41] proved unsuccessful, likely due to steric congestion imposed by the heptafluoroisopropyl group, which disfavors benzylic deprotonation. To circumvent this barrier, we envisioned replacing the sulfonate with a less sterically demanding substituent prior to elimination. Screening identified $MgBr_2$ as uniquely effective in promoting sulfonate displacement (Scheme 2b) (for details, see the Supporting Information Table S3). In contrast, analogous benzenesulfonates exhibited substantially lower reactivity, highlighting the key role of pyridyl nitrogen coordination in facilitating magnesium-mediated substitution. Notably, switching the solvent from DMF to MeCN enabled direct bromination following formal insertion of aldehyde. Under optimized conditions, bromide intermediate **4f** was isolated in 85% yield. Subsequent treatment with LiHMDS furnished bromo-*gem*-bis(trifluoromethyl) alkene **5f** in 77% yield. These findings established a mechanistically required bromination-elimination sequence, converting an otherwise unreactive sulfonate into a synthetically versatile brominated alkene scaffold.

Citation: *CCS Chem.* **2026**, Just Published. DOI: 10.31635/ccschem.026.202608038
Link to VoR: https://doi.org/10.31635/ccschem.026.202608038



Scheme 2 | *HFIPS-enabled aldehyde olefination: isolated intermediates, stepwise validation, and one-pot scope. (a) HFIPS addition to aldehydes: isolated sulfonate intermediates; (b) olefination validated through bromination of sulfonate intermediates; (c) one-pot olefination of aldehydes to tetrasubstituted alkenes. Yields refer to isolated products. Yields determined by ^{19}F NMR analysis are shown in the parentheses. [a]Reactions were conducted on a 0.50 mmol scale:* ***1*** *(1.0 equiv) and aldehyde* ***2*** *(1.0 equiv) in MeCN (0.1 M) with CsF (0.2 equiv) at RT for 4 h; then $MgBr_2 \cdot Et_2O$ (2.0 equiv) at 80 °C for 12 h; after filtration and solvent removal, Et_2O (10 mL), HMPA (1.0 mL), and LiHMDS (1.5 equiv) were added at 0 °C for 30 min under N_2. LiHMDS = Lithium bis(trimethylsilyl)amide; HMPA = hexamethylphosphoramide.*

Citation: *CCS Chem.* **2026**, Just Published. DOI: 10.31635/ccschem.026.202608038
Link to VoR: https://doi.org/10.31635/ccschem.026.202608038

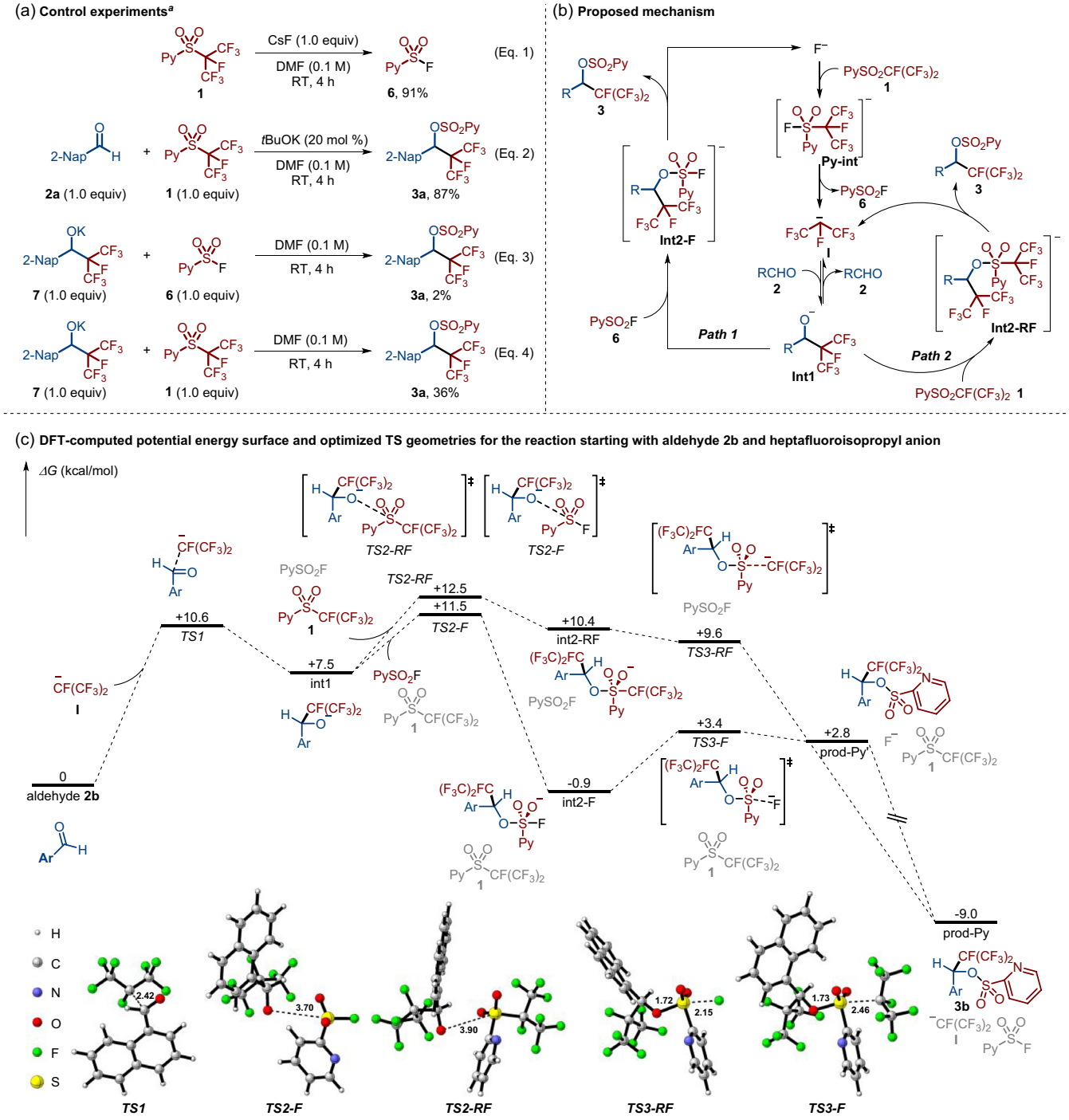
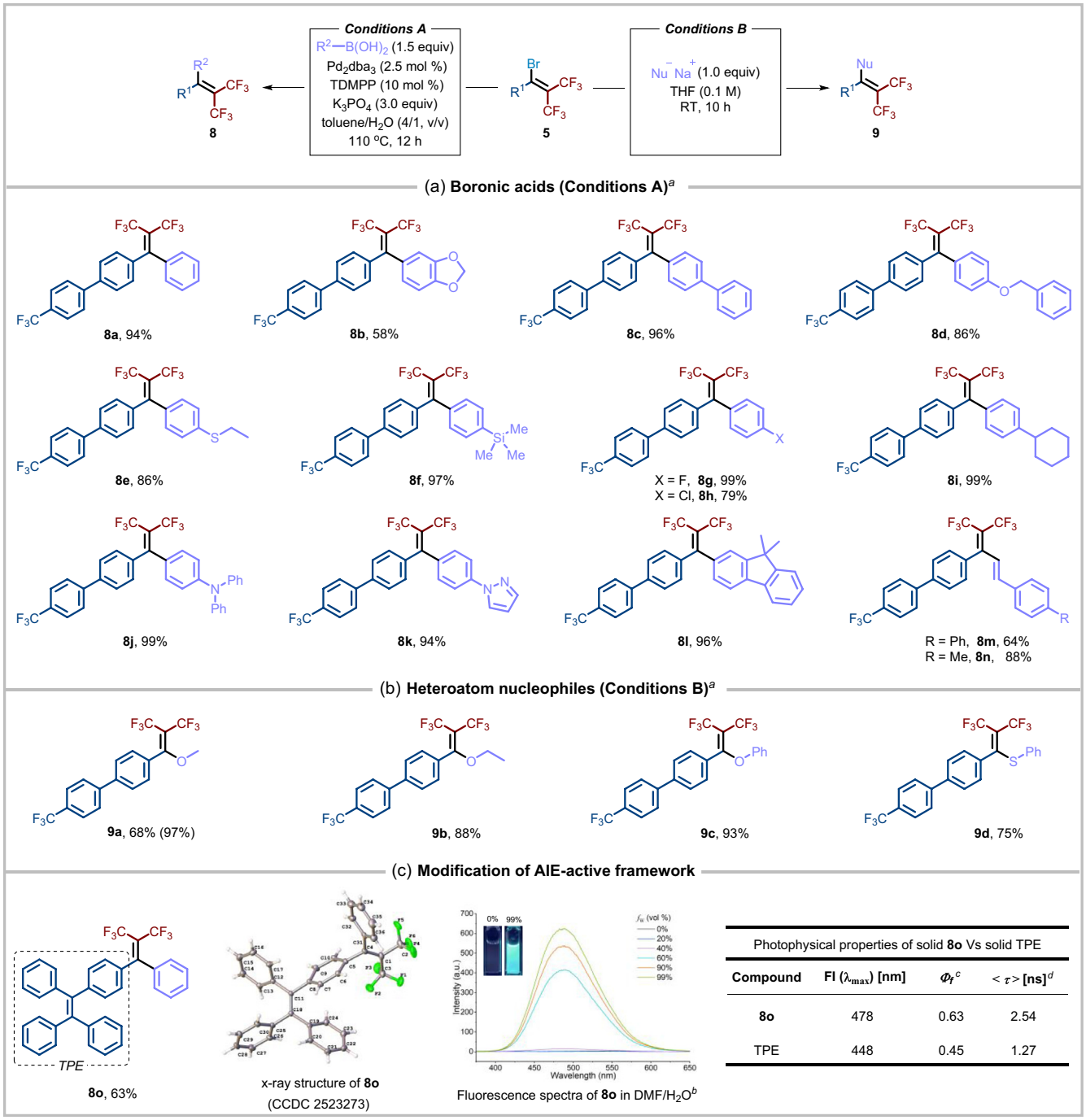


Figure 2 | *Mechanistic investigation and reaction coordinate diagram for HFIPS addition to aldehydes. (a) Control experiments. (b) Proposed mechanism. (c) DFT-computed potential energy surface and optimized TS geometries for the reaction starting with aldehyde* ***2b*** *and heptafluoroisopropyl anion.*[a]

Development of a one-pot olefination protocol

Building on these insights, a streamlined one-pot process integrating formal insertion of aldehyde, magnesium-mediated bromination, and base-induced elimination was developed (Scheme 2c). The olefination proceeded efficiently with electronically neutral (**5a**–**5e**, **5i**, **5j**), moderately electron-rich (**5h**), and moderately electron-deficient (**5f**, **5g**) aryl aldehydes. Strongly electron-deficient substrates (**3n**), sterically encumbered electron-deficient aldehydes (**3l**), and aliphatic aldehydes (**3o**) were ineffective due to inefficient bromination. These limitations reflect the combined steric and electronic constraints inherent to the

Citation: *CCS Chem.* **2026**, Just Published. DOI: 10.31635/ccschem.026.202608038
Link to VoR: https://doi.org/10.31635/ccschem.026.202608038



Photophysical properties of solid **8o** Vs solid TPE

Compound	Fl (λ_{max}) [nm]	Φ_f [c]	$<\tau>$ [ns] [d]
8o	478	0.63	2.54
TPE	448	0.45	1.27

Scheme 3 | *Downstream functionalization and materials application. (a) Boronic acids (Conditions A). (b) Heteroatom nucleophiles (Conditions B). (c) Modification of AIE-active framework.[a]Reactions were conducted on a 0.10 mmol scale. Yields refer to isolated products. Yields determined by ^{19}F NMR analysis are shown in the parentheses. [b]Fluorescence spectra of **8o** (1.0×10^{-4} M) in DMF upon the addition of various amounts of water (λ_{ex} = 330 nm). Inset: photographs of **8o** solutions in DMF and DMF/water (v/v = 1:99) under UV illumination (365 nm). [c]The fluorescence quantum yield (Φ_f) was measured using a calibrated integrating sphere. [d]An apparent fluorescence decay time constant ($<\tau>$) was determined using the equation $<\tau> = \Sigma(A_i \times \tau_i)/\Sigma A_i$ (i = 1–n, n = 2), where τ_i and A_i represent the individual exponential decay time constants and their corresponding pre-exponential factors, respectively (for details, see Supporting Information Figures S8–S13, and Table S7). dba = dibenzylideneacetone; TDMPP = Tris(2,6-dimethoxyphenyl)phosphine; TPE = tetraphenylethene; Fl = fluorescence.*

Citation: *CCS Chem.* **2026**, Just Published. DOI: 10.31635/ccschem.026.202608038
Link to VoR: https://doi.org/10.31635/ccschem.026.202608038

mechanistically essential bromination-elimination sequence. To our knowledge, no general synthetic strategy for accessing brominated *gem*-bis(trifluoromethyl) alkenes of this type has been previously reported.

Downstream functionalization and materials application

Importantly, bromination is mechanistically indispensable for enabling the olefination sequence while simultaneously introducing a versatile functional handle for downstream diversification. The synthetic versatility of the resulting brominated alkenes was further demonstrated (Scheme 3).

Under Suzuki coupling conditions,[42] model substrate **5f** reacted smoothly with aryl and vinyl boronic acids to furnish unsymmetrical tetrasubstituted *gem*-bis(trifluoromethyl) alkenes (**8a**–**8n**) (Scheme 3a). In contrast, Suzuki coupling of 1,1-dibromo-3,3,3-trifluoro-2-(trifluoromethyl)prop-1-ene ($Br_2C=C(CF_3)_2$) typically proceeds through rapid double cross-coupling, affording only symmetrical diaryl alkenes.[43] Selective monocoupling cannot be achieved, precluding stepwise introduction of two different aryl groups. These observations underscore the strategic advantage of the monobrominated intermediates, which enables controlled sequential functionalization and access to unsymmetrical *gem*-bis(trifluoromethyl)olefin architectures. The monobrominated alkenes also underwent nucleophilic substitution with sodium alkoxides, phenolates, and thiolates to afford structurally diverse heteroatom-substituted tetrasubstituted alkenes (**9a**–**9d**) (Scheme 3b). In contrast, sterically demanding nucleophiles such as sodium isopropoxide or *tert*-butoxide were ineffective. This pronounced steric discrimination may be exploited for chemoselective transformations in complex molecules bearing multiple nucleophilic sites.

To illustrate its potential in materials chemistry, a tetraphenylethene (TPE)-derived aldehyde was subjected to the olefination/Suzuki sequence to furnish compound **8o**, a stable AIE-active molecule with markedly enhanced quantum yield (0.45→0.63) and prolonged emission lifetime versus simple TPE[44–47] (Scheme 3c). Single-crystal analysis of **8o** (for details, see Supporting Information Figure S7 and Table S6) reveals that all phenyl rings directly attached to the double bond adopt highly twisted dihedral angles with the adjacent double bond (67.2° and 70.4° for the $(CF_3)_2C=C$ unit; 44.7°–65.7° for the 4-TPE unit, slightly larger than 47°–58° in simple TPE[48]), reflecting enhanced restricted intramolecular rotation.[47] The TPE core shows inter-phenyl angles ranging from 51.1° to 85.8°, more dispersed than in simple TPE (54.3°–80.0°),[48] indicating a modest increase in overall rigidity.[47] These structural features demonstrate that CF_3-induced local twisting, together with slightly increased core rigidity, suppresses intramolecular rotation, leading to reduced non-radiative decay. Consequently, long-lived emission components and apparent decay constants (<τ>) are enhanced, rationalizing the pronounced AIE behavior.

Conclusions

In summary, we report a HFIPS-enabled strategy that unlocks fluoride-triggered formal insertion of aldehyde into C–S bonds, overcoming the intrinsic limitations of conventional fluoroalkyl sulfones. Mechanistic studies reveal that aldehyde addition is rate-determining and identify HFIPS as the operative sulfonylating species under catalytic fluoride activation. A mechanistically indispensable bromination-elimination sequence enables efficient access to tetrasubstituted *gem*-bis(trifluoromethyl) alkenes under mild conditions. The resulting monobrominated intermediates provide a versatile handle for modular downstream functionalization. Structural and photophysical analyses demonstrate that CF_3-induced steric restriction enhances solid-state AIE behavior. Collectively, this work establishes a unified platform linking formal C–S insertion chemistry with fluorinated alkene synthesis and functional materials development.

Supporting Information

Supporting Information is available and includes details on experimental procedures, reaction optimizations, mechanistic investigation of the addition reaction, X-ray crystallographic analysis, AIE studies, and compound characterization data.

Conflict of Interest

There is no conflict of interest to report.

Funding Information

Financial support of this work by the Strategic Priority Research Program of the Chinese Academy of Sciences (grant no. XDB0590000), the National Natural Science Foundation of China (grant no. 22271299), and the Natural Science Foundation of Shandong Province (grant no. ZR2023LFG003) is gratefully acknowledged.

References

1. Lu, M.-Z.; Goh, J.; Maraswami, M.; Jia, Z.; Tian, J.-S.; Loh, T.-P. Recent Advances in Alkenyl sp^2 C–H and C–F Bond Functionalizations: Scope, Mechanism, and Applications. *Chem. Rev.* **2022**, *122*, 17479–17646.

Citation: *CCS Chem.* **2026**, Just Published. DOI: 10.31635/ccschem.026.202608038
Link to VoR: https://doi.org/10.31635/ccschem.026.202608038

2. Ertl, P.; Schuhmann, T. A Systematic Cheminformatics Analysis of Functional Groups Occurring in Natural Products. *J. Nat. Prod.* **2019**, *82*, 1258–1263.
3. Takeda, T. *Modern Carbonyl Olefination*. Wiley-VCH, Weinheim, **2019**.
4. Albright, H.; Davis, A. J.; Gomez-Lopez, J. L.; Vonesh, H. L.; Quach, P. K.; Lambert, T. H.; Schindler, C. S. Carbonyl–Olefin Metathesis. *Chem. Rev.* **2021**, *121*, 9359–9406.
5. Bongso, A.; Roswanda, R.; Syah, Y. M. Recent Advances of Carbonyl Olefination via McMurry Coupling Reaction. *RSC Adv.* **2022**, *12*, 15885–15909.
6. Aïssa, C. Mechanistic Manifold and New Developments of the Julia–Kocienski Reaction. *Eur. J. Org. Chem.* **2009**, *2009*, 1831–1844.
7. Blakemore, P. R. The Modified Julia Olefination: Alkene Synthesis via the Condensation of Metallated Heteroarylalkylsulfones with Carbonyl Compounds. *J. Chem. Soc. Perkin Trans.* **2002**, *1*, 2563–2585.
8. Sakaine, G.; Leitis, Z.; Ločmele, R.; Smits, G. Julia-Kocienski Olefination: A Tutorial Review. *Eur. J. Org. Chem.* **2023**, *26*, e202201217.
9. Ouzounthanasis, K. A.; Rizos, S. R.; Koumbis, A. E. Julia-Kocienski Olefination in the Synthesis of Trisubstituted Alkenes: Recent Progress. *Eur. J. Org. Chem.* **2023**, *26*, e202300626.
10. Chrenko, D.; Pospíšil, J. Latest Developments of the Julia–Kocienski Olefination Reaction: Mechanistic Considerations. *Molecules* **2024**, *29*, 2719.
11. Zhao, Y.; Huang, W.; Zhu, L.; Hu, J. Difluoromethyl 2-Pyridyl Sulfone: A New *gem*-Difluoroolefination Reagent for Aldehydes and Ketones. *Org. Lett.* **2010**, *12*, 1444–1447.
12. Zajc, B.; Kumar, R. Synthesis of Fluoroolefins via Julia-Kocienski Olefination. *Synthesis* **2010**, *2010*, 1822–1836.
13. Ni, C.; Hu, M.; Hu, J. Good Partnership Between Sulfur and Fluorine: Sulfur-Based Fluorination and Fluoroalkylation Reagents for Organic Synthesis. *Chem. Rev.* **2015**, *115*, 765–825.
14. Chu, X.-Q.; Ge, D.; Cui, Y.-Y.; Shen, Z.-L.; Li, C.-J. Desulfonylation via Radical Process: Recent Developments in Organic Synthesis. *Chem. Rev.* **2021**, *121*, 12548–12680.
15. Nambo, M.; Maekawa, Y.; Crudden, C. M. Desulfonylative Transformations of Sulfones by Transition-Metal Catalysis, Photocatalysis, and Organocatalysis. *ACS Catal.* **2022**, *12*, 3013–3032.
16. Corpas, J.; Kim-Lee, S.-H.; Mauleón, P.; Arrayás, R. G.; Carretero, J. C. Beyond Classical Sulfone Chemistry: Metal- and Photocatalytic Approaches for C–S Bond Functionalization of Sulfones. *Chem. Soc. Rev.* **2022**, *51*, 6774–6823.
17. Wang, X.; Hu, J. Sulfur-Based Organofluorine Reagents for Selective Fluorination, Fluoroalkylation, and Fluoroolefination Reactions. *Phosphorus, Sulfur, and Silicon and the Relat. Elem.* **2024**, *199*, 10–22.
18. Prakash, G. K. S.; Knieb, A. Recent Advances in Fluoroalkylation Strategies: Exploring Novel Reactivities and Synthetic Applications of Sulfone- and Sulfinate-Based Reagents for Mono-, Di-, and Trifluoromethylations. *Synthesis* **2025**, *57*, 331–361.
19. Shlapakov, N. S.; Kobelev, A. D.; Burykina, J. V.; Cheng, Y.-Z.; You, S.-L.; Ananikov, V. P. Sulfur in Waste-Free Sustainable Synthesis: Advancing Carbon–Carbon Coupling Techniques. *Angew. Chem. Int. Ed.* **2024**, *63*, e202402109.
20. Dong, J.; Krasnova, L.; Finn, M. G.; Sharpless, K. B. Sulfur(VI) Fluoride Exchange (SuFEx): Another Good Reaction for Click Chemistry. *Angew. Chem. Int. Ed.* **2014**, *53*, 9430–9448.
21. Liu, C.; Yang, C.; Hwang, S.; Ferraro, S. L.; Flynn, J. P.; Niu, J. A General Approach to *O*-Sulfation by a Sulfur(VI) Fluoride Exchange Reaction. *Angew. Chem. Int. Ed.* **2020**, *59*, 18435–18441.
22. Lou, T. S.-B.; Willis, M. C. Sulfonyl Fluorides as Targets and Substrates in the Development of New Synthetic Methods. *Nat. Rev. Chem.* **2022**, *6*, 146–162.
23. Smedley, C. J.; Zheng, Q.; Gao, B.; Li, S.; Molino, A.; Duivenvoorden, H. M.; Parker, B. S.; Wilson, D. J. D.; Sharpless, K. B.; Moses, J. E. Bifluoride Ion Mediated SuFEx Trifluoromethylation of Sulfonyl Fluorides and Iminosulfur Oxydifluorides. *Angew. Chem. Int. Ed.* **2019**, *58*, 4552–4556.
24. Wei, Z.; Wen, L.; Zhu, K.; Wang, Q.; Zhao, Y.; Hu, J. Regioselective Aromatic Perfluoro-tert-butylation Using Perfluoro-*tert*-Butyl Phenyl Sulfone and Arynes. *J. Am. Chem. Soc.* **2022**, *144*, 22281–22288.
25. Zhu, K.; Luo, Q.; Xu, P.; Ni, Z.; Sun, S.; Hu, M.; Ni, C.; Hu, J. Dehydroxy-Perfluoro-*tert*-Butylation of Alcohols with $PhSO_2C(CF_3)_3$ and Insights into the Structure of the $[C(CF_3)_3]^-$ Anion. *Nat. Commun.* **2025**, *16*, 7969.
26. Jarvis, B. B.; Tong, W. P.; Ammon, H. L. Reactions of 2,3-Diphenylthiirene 1,1-Dioxide with Nucleophiles. *J. Org. Chem.* **1975**, *40*, 3189–3195.
27. Eleev, A. F.; Sokol'Skii, G. A.; Knunyants, I. L. Fluorinated β-Sultones 46. 2-Hydrohexafluoropropane-2-Sulfofluoride. *Russ. Chem. Bull.* **1977**, *26*, 1444–1448.
28. Smart, B. E.; Middleton, W. J. Bis(trifluoromethyl)Sulfene: Generation and Cycloaddition Reactions. *J. Am. Chem. Soc.* **1987**, *109*, 4982–4992.
29. Hartwig, U.; Rall, K.; Sundermeyer, W. Bis(trifluormethyl)Sulfen, $(CF_3)_2C = SO_2$: Seine Darstellung und Isolierung als Amin-Addukt. *Chem. Ber.* **1990**, *123*, 595–598.
30. Kirmse, W. Intermediates of α-Eliminations. *Angew. Chem. Int. Ed.* **1965**, *4*, 1–10.
31. Gessner, V. H. Stability and Reactivity Control of Carbenoids: Recent Advances and Perspectives. *Chem. Commun.* **2016**, *52*, 12011–12023.
32. Zhang, W.; Ni, C.; Hu, J. Selective Fluoroalkylation of Organic Compounds by Tackling the "Negative Fluorine Effect". *Top. Curr. Chem.* **2012**, *308*, 25.
33. Liu, Y.; Wang, X.; Ni, C.; Hu, J. Nucleophilic Trifluoromethylation with CF_3H/LiHMDS: Probing the Nucleophilic Reactivity of $LiCF_3$ Species. *Sci. China Chem.* **2025**, *68*, 505–512.
34. Mayr, H.; Ofial, A. R. Do General Nucleophilicity Scales Exist? *J. Phys. Org. Chem.* **2008**, *21*, 584–595.

Citation: *CCS Chem.* **2026**, Just Published. DOI: 10.31635/ccschem.026.202608038
Link to VoR: https://doi.org/10.31635/ccschem.026.202608038

35. Furukawa, T.; Goto, Y.; Kawazoe, J.; Tokunaga, E.; Nakamura, S.; Yang, Y.; Du, H.; Kakehi, A.; Shiro, M.; Shibata, N. 2-Fluoro-1,3-benzodithiole-1,1,3,3-tetraoxide: A Reagent for Nucleophilic Monofluoromethylation of Aldehydes. *Angew. Chem. Int. Ed.* **2010**, *49*, 1642–1647.
36. Shen, X.; Ni, C.; Hu, J. Nucleophilic Fluoroalkylation of α,β-Unsaturated Carbonyl Compounds with α-Fluorinated Sulfones: Investigation of the Reversibility of 1,2-Additions and the Formation of 1,4-Adducts. *Helv. Chim. Acta* **2012**, *95*, 2043–2051.
37. Hanessian, S.; Kagotani, M.; Komaglou, K. Design a nd Reactivity of Organic Functional Groups—2-Pyridylsulfonates as Nucleofugal Esters: Remarkably Mild Transformations into Halides and Olefins. *Heterocycles* **1989**, *28*, 1115.
38. Wang, Q.; Ni, C.; Hu, M.; Xie, Q.; Liu, Q.; Pan, S.; Hu, J. From C_1 to C_3: Copper-Catalyzed *gem*-Bis(trifluoromethyl) Olefination of α-Diazo Esters with $TMSCF_3$. *Angew. Chem. Int. Ed.* **2020**, *59*, 8507–8511.
39. Prakash, G. K. S.; Hu, J.; Olah, G. A. Alkoxide- and Hydroxide-Induced Nucleophilic Trifluoromethylation Using Trifluoromethyl Sulfone or Sulfoxide. *Org. Lett.* **2003**, *5*, 3253–3256.
40. Prakash, G. K. S.; Wang, Y.; Mogi, R.; Hu, J.; Mathew, T.; Olah, G. A. Nucleophilic Perfluoroalkylation of Imines and Carbonyls: Perfluoroalkyl Sulfones as Efficient Perfluoroalkyl-Transfer Motifs. *Org. Lett.* **2010**, *12*, 2932–2935.
41. Ignatowska, J.; Dmowski, W. Sodium Dithionite Initiated Addition of CF_2Br_2, CF_3I and $(CF_3)_2CFI$ to Allylaromatics: Synthesis and the Reactivity of 4-aryl-1,1-Difluorodienes and 4-aryl-1,1-bis(trifluoromethyl)Dienes. *J. Fluorine Chem.* **2007**, *128*, 997–1006.
42. Suzuki, A. Cross-Coupling Reactions of Organoboranes: An Easy Way To Construct C–C Bonds (Nobel Lecture). *Angew. Chem. Int. Ed.* **2011**, *50*, 6722–6737.
43. Wang, Q. Shanghai Institute of Organic Chemistry, University of Chinese Academy of Sciences, Ph D. thesis, CAS (CN) **2020**.
44. Liu, J.; Zhang, H.; Hu, L.; Wang, J.; Lam, J. W. Y.; Blancafort, L.; Tang, B. Z. Through-Space Interaction of Tetraphenylethylene: What, Where, and How. *J. Am. Chem. Soc.* **2022**, *144*, 7901–7910.
45. Gu, X.; Yao, J.; Zhang, G.; Zhang, C.; Yan, Y.; Zhao, Y.; Zhang, D. New Electron-Donor/Acceptor-Substituted Tetraphenylethylenes: Aggregation-Induced Emission with Tunable Emission Color and Optical-Waveguide Behavior. *Chem. Asian J.* **2013**, *8*, 2362–2369.
46. Mei, J.; Hong, Y.; Lam, J. W. Y.; Qin, A.; Tang, Y.; Tang, B. Z. Aggregation-Induced Emission: The Whole is More Brilliant Than the Parts. *Adv. Mater.* **2014**, *26*, 5429–5479.
47. Mei, J.; Leung, N. L. C.; Kwok, R. T. K.; Lam, J. W. Y.; Tang, B. Z. Aggregation-Induced Emission: Together We Shine, United We Soar! *Chem. Rev.* **2015**, *115*, 11718–11940.
48. Zhang, S.; Ma, F.; Jiang, J.; Wu, B.; Gong, J.; Xu, G.; Li, C.; Chen, T.; Kwok, R. T. K.; Lam, J. W. Y.; Zhao, Z.; Tang, B. Z. Isotope Engineering of Tetraphenylethylene: Aggregate-Dependent Enhancement of Luminescence Efficiency. *Angew. Chem. Int. Ed.* **2025**, *64*, e202511678.

Citation: *CCS Chem.* **2026**, Just Published. DOI: 10.31635/ccschem.026.202608038
Link to VoR: https://doi.org/10.31635/ccschem.026.202608038